CHALMERS
UNIVERSITY OF TECHNOLOGY

Joint Detection and Localization of Multiple Moving Targets in a Distributed Radar System

Citation for the original published paper (version of record):
Lai, Y., Yi, W., Wymeersch, H. et al (2024). Joint Detection and Localization of Multiple Moving Targets in a Distributed Radar System. IEEE Sensors Journal, 24(17): 27914-27925.
http://dx.doi.org/10.1109/JSEN.2024.3432636

(article starts on next page)

Joint Detection and Localization of Multiple Moving Targets in a Distributed Radar System

Yangming Lai, *Student Member, IEEE*, Wei Yi, *Senior Member, IEEE*, Henk Wymeersch, *Fellow, IEEE*, Musa Furkan Keskin, *Member, IEEE*, Qiyu Zhou, and Lingjiang Kong, *Senior Member, IEEE*

***Abstract*— This article investigates the joint detection and localization (JDL) problem of unknown number multiple moving targets in a distributed radar system. Upon formulating this problem as a composite multiple hypothesis testing problem, we derive a generalized information criterion (GIC)-based detector to simultaneously extract targets and estimate their unknown parameters, including their number, amplitudes, locations, and velocities. Although this solution theoretically achieves impressive performance by using raw echoes data to jointly detect and estimate multiple targets at the fusion center (FC), it also requires an unbearable computational load in practice. It is because multiple targets are expected to be simultaneously extracted by realizing a joint maximization task and making an enormous search. To reduce the computational burden, we propose a low-complexity solution to decompose the high-dimensional problem into several low-dimensional optimization problems. For local radars to undertake a portion of the calculations, the log-likelihood ratio (LLR) data are generated at each local station and then completely transmitted to the FC. Different from extracting multiple targets simultaneously using a GIC-based detector, we devise an extended successive-interference-cancellation (SIC) algorithm to detect targets one by one at the FC, and meanwhile, the parameters of targets can be simultaneously estimated at each iteration. Finally, the effectiveness of the proposed algorithm is demonstrated by the provided simulations.**

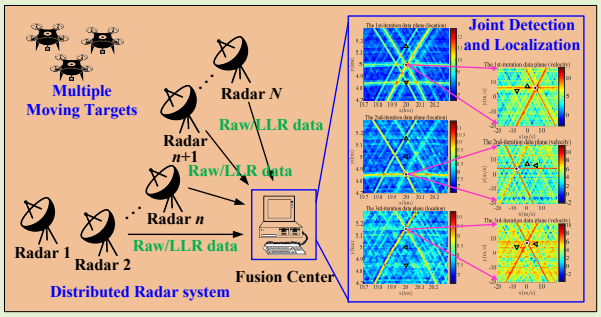

***Index Terms*— Distributed radar system, joint detection and localization, generalized likelihood ratio test, iterative cancellation, generalized information criterion.**

I. Introduction

With the rapid advancements in radar technology, there has been significant interest in distributed radar systems [1]–[3], spanning both military and civilian domains [4], [5]. Compared with a single monostatic radar, a distributed radar system offers several advantages: it exhibits greater immunity to jamming owing to the distributed placement of multiple radar sensor nodes [6]; it provides additional stability, reliability, and degrees of freedom [7]; it offers a wide field of view by observing targets from different angles, thereby introducing spatial diversity and effectively mitigating the effects of target radar cross-section (RCS) fading [8]. Therefore, a distributed radar system can achieve enhanced performance of target imaging [9], detection [10], [11], localization [12], [13], classification [14], and tracking [15], [16]. Among them, target detection and localization are the fundamental functions of radar sensors [17]–[19]. In general, there are two primary approaches for achieving target detection and/or localization in the broad array of applications involving distributed radar systems [20].

The first category of approaches involves a two-step process for detection and localization [21]–[24]. Initially, each radar node performs preliminary detection and estimation. Subsequently, the local detection decisions, represented as '$0/1$' to denote not detected or detected, as well as the estimated position measurements such as angle of arrival (AOA) [22] and time of arrival (TOA) [23], [24], are transmitted to a fusion center (FC). Finally, the FC performs global decision-making utilizing detection rules such as 'AND', 'OR', or 'M out of N' [25] for detection and employs pairing and triangulation of the extracted parameters for localization [26], [27]. Besides, the works in [28] and [29] investigate joint detection and tracking algorithms for distributed radars. These algorithms transmit the estimated range, Doppler, and AOA measurements to the FC and utilize the resulting tracking results to adjust local

The work of Yangming Lai, Wei Yi, Qiyu Zhou, and Lingjiang Kong was supported by the National Natural Science Foundation of China under Grant 62231008 and 62301127. The work of Henk Wymeersch and Musa Furkan Keskin was supported by the SNS JU project 6G-DISAC under the EU's Horizon Europe research and innovation Program under Grant Agreement No 101139130. (*Corresponding author: Wei Yi.*)

Yangming Lai, Wei Yi, Qiyu Zhou, and Lingjiang Kong are with the School of Information and Communication Engineering, University of Electronic Science and Technology of China, Chengdu 611731, China (e-mail: ymlai1996@gmail.com; kussoyi@gmail.com; qiyuzhou2018@gmail.com; ljkong@uestc.edu.cn).

Henk Wymeersch and Musa Furkan Keskin are with the Department of Electrical Engineering, Chalmers University of Technology, 41296, Gothenburg, Sweden (email: henkw@chalmers.se; furkan@chalmers.se).

radar thresholds, thereby enhancing detection and tracking performance. In summary, this category entails a relatively low computational burden and transmission bandwidth between local nodes and the FC. However, it may lead to a significant drop in detection and localization performance due to the simplified extraction of the information of the raw echoes data, particularly the occurrence of missed detections, false alarms, and/or estimation errors at certain local stations.

The second category, primarily considered in this paper, involves the direct and joint processing of raw local echoes or log-likelihood ratio (LLR) data at the FC for target detection [30], [31] and/or localization [32]–[34]. This approach offers superior performance as it avoids making preliminary decisions locally at each radar, which corresponds to the former category. It also leads to enhanced robustness in detection and localization performance, especially in scenarios characterized by low signal-to-noise ratio (SNR). The existing literature on this topic can be categorized into two cases, as follows.

1) *Case 1: Separate detection or localization:* The studies in [35]–[39] implement target detection based on the generalized likelihood ratio test (GLRT) considering different problems in distributed multiple-input multiple-output (MIMO) radar systems. Meanwhile, [32]–[34] realize localization without detection by utilizing maximum likelihood estimations (MLEs) of the unknown parameters. Low-bit quantization algorithms are proposed in [40] and [41] for addressing hybrid quantized signal detection and direct localization, respectively. Besides, geometric matching and spatial mapping algorithms are introduced in [42] and [43] to address the detection problems of multiple stationary and moving targets, respectively.
2) *Case 2: Joint detection and localization (JDL):* Differing from the former case realizing individual function, implementing simultaneous detection and localization in distributed radar systems when probing multiple targets has gained significant traction recently [44]–[49]. This case aims to directly estimate unknown target locations in the state space while utilizing detection thresholds to ensure the reliability of the estimates. Once a detection is declared, the target location in the Cartesian coordinate system will be output. As a foundational work in the JDL for distributed radars, [44] introduces a novel framework for jointly detecting the presence of a single stationary target and estimating its unknown parameters. In [45], a JDL algorithm is proposed to localize a single stationary target once its presence is declared. In [46] and [47], different iterative cancellation algorithms are proposed to achieve the JDL of multiple stationary targets, utilizing ideal and imperfect auto- and cross-correlation waveform functions, respectively. An energy-guided framework is also proposed in [48] to address the JDL of stationary targets. Besides, a compressed sensing-based framework achieves the enumeration and localization of stationary targets with reduced communication load in [49].

However, the JDL works discussed in Case 2 predominantly focus on stationary targets in distributed radar systems. In reality, targets are often in motion, resulting in Doppler shifts across multiple pulses. Efficiently detecting multiple moving targets and directly estimating their parameters utilizing raw echoes or LLR data at the FC remains a complex and unsolved problem. It should be noted that, there are also joint detection and estimation works (e.g., [50]–[53]) that investigate different problems in single radar systems, such as phase-array radar [50]–[52] or colocated MIMO radar [53]. As noted in [53], the paper [50] is seminal in this field. These works focus on detecting targets and outputting the corresponding ranges, angles, and Doppler shifts as by-products [53]. Due to the characteristics of single radar systems, further calculations are required to determine corresponding target locations and velocities in the Cartesian coordinate system.

In this paper, a low-complexity solution is introduced to realize the JDL of multiple moving targets in distributed radar systems. Consistent with the design principles of our previous works on multiple stationary targets [46], [47], an iterative algorithm is developed to detect multiple moving targets sequentially. At each iteration, upon the LLR data of the previously detected targets being eliminated, this algorithm directly and simultaneously outputs the corresponding locations and velocities in the Cartesian coordinate system once the next target is declared. The main contributions are summarized as follows:

- We first formulate a novel JDL problem for multiple moving targets as a composite multiple-hypothesis testing problem. We then derive a detector based on generalized information criterion (GIC) to simultaneously detect the targets and estimate their number, amplitudes, locations, and velocities at the FC.
- Considering the high computational burden of the derived detector due to simultaneously extracting multiple targets by realizing a joint maximization task and making the enormous search. We then propose a low-complexity solution to decompose the high-dimensional joint maximization task into several low-dimensional optimization steps. At the FC, an extended successive-interference-cancellation (SIC) algorithm is devised to extract one target per time and eliminate its LLR data. Meanwhile, the parameters of targets can be simultaneously obtained at each iteration.
- We conduct a numerical study to validate the efficacy of the proposed algorithm. The results confirm that our procedure can correctly detect targets one by one and simultaneously estimate the location and velocity of a target at each iteration, upon eliminating the LLR data of the previously detected targets.

This paper is organized as follows. Section II presents the system and signal model. Section III formulates the JDL problem of multiple moving targets. The proposed low-complexity solution is described in Section IV. Section V provides the simulation results to demonstrate the effectiveness of the proposed algorithm. Finally, conclusions are provided in Section VI.

Notations: Lowercase and uppercase boldface letters de-

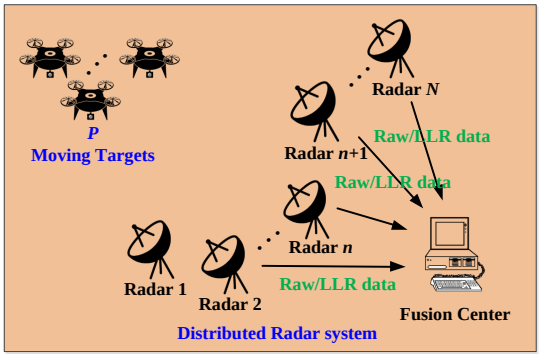

Fig. 1. Illustration of a distributed radar system with N local stations and P moving targets. There exists a communication system without distortion, enabling the FC to flawlessly gather the complete raw data from each local station.

note Column vectors and matrices, respectively, whereas the conjugate, transpose, and conjugate-transpose operations are denoted by $(\cdot)^*$, $(\cdot)^\top$, and $(\cdot)^H$, respectively. Furthermore, $\|\boldsymbol{a}\|$ is the Euclidean norm of the vector $\boldsymbol{a}$. Additionally, cat$\{\boldsymbol{a}_1,\ldots,\boldsymbol{a}_Y\}$ forms an MY-dimensional vector by concatenating the M-dimensional vectors $\{\boldsymbol{a}_n\}_{n=1}^Y$, and the $M\times M$ identity matrix is represented by $\mathbf{I}_M$. Finally, $\jmath$, $\otimes$, and $+$ denote the imaginary unit, Kronecker product, and the pseudoinverse operator, respectively, while $\lceil\cdot\rceil$ and $\mathbb{E}\{\cdot\}$ represent the function rounding upwards and the statistical expectation.

II. System and Signal Model

Consider a distributed radar system with N local stations located at $\{\boldsymbol{x}_n\}_{n=1}^N \in \mathbb{R}^2$ and P point-like [50] moving targets initially located at $\boldsymbol{\theta}_p \in \mathbb{R}^2$ with constant velocities $\boldsymbol{v}_p \in \mathbb{R}^2$ ($p=1,...,P$, and P is an a-priori unknown variable), in a two dimensional Cartesian coordinate system. It is assumed that all stations can observe all the targets, share a common time reference and operate within the same spectrum, and there exists a communication system without distortion, enabling the FC to flawlessly gather the complete raw data from each local station, as illustrated in Fig. 1.

A. Transmit Signal Model

Firstly, the transmitted baseband signal of each local station for a pulse repetition interval (PRI) is denoted by

$$s_n(t) = \sqrt{E/N}x_n(t)W(t) \tag{1}$$

where $n=1,\ldots,N$, $0<t\le T_{\text{pri}}$, T_{pri} represents the duration of a PRI, and E is the total transmitted energy; $W(t)$ is a rectangular window, i.e.,

$$W(t) = \begin{cases} 1, & 0<t\le T_{\text{pri}} \\ 0, & \text{otherwise.} \end{cases} \tag{2}$$

Then, the lowpass-equivalent waveforms $\{x_n(t)\}_{n=1}^N$ are assumed to be time-limited to $(0,\mathcal{T}_d]$ and essentially frequency limited to $[-B/2,B/2]$ [47], [54], where $\mathcal{T}_d \le T_{\text{pri}}$ denotes the duration of the waveform. An assumption is made that the orthogonality of the transmitted signals is approximately maintained for any time delay τ of interest, i.e.,

$$\int_{\mathcal{T}_d} x_{n_1}(t)x_{n_2}^*(t-\tau)dt = \begin{cases} 1, & n_1=n_2 \\ \epsilon, & \text{otherwise} \end{cases} \tag{3}$$

where ϵ is the cross-correlation value ($n_1\neq n_2$, $n_1,n_2=1,...,N$) which can be assumed as $\epsilon\approx 0$ when suitable waveform design techniques are applied in practice [46].

B. Received Signal Model

We assume all transmitted signals are observed and ignore range migration in a single coherent processing interval (CPI) which contains Y PRIs, i.e., the duration of a CPI is $T_{\text{cpi}}=YT_{\text{pri}}$. Then, the received y-th signal ($y=1,\ldots,Y$), which is reflected upon P moving targets, observed, downconverted, and matched-filtered by the n-th station, can be accurately represented as

$$r_{n,y}(t) = \sum_{p=1}^{P}\alpha_{n,p}\overline{s}_n\left(t-\tau_{n,p}\right)e^{\jmath 2\pi f_{n,p}(y-1)T_{\text{pri}}} + w_{n,y}(t) \tag{4}$$

where $p=1,\ldots,P$, and $\alpha_{n,p}$ is the complex reflection coefficient of the p-th target at the n-th station; the term $\overline{s}_n(t)$ denotes the matched filtering output signal of $s_n(t)$ by employing the n-th transmitted waveform $x_n(t)$, it has a narrow-pulse property in time domain and the auto-terms $\overline{s}_n(t-\tau_{n,p})$ and $\overline{s}_n(t-\tau_{n,q})$ are orthogonal if $(\tau_{n,p}\neq\tau_{n,q})$ [46, eq. (27) and footnote 4][1]. The noise term $w_{n,y}(t)$ is modeled as complex circularly symmetric Gaussian noise with the independent zero-mean property and intensity σ_w^2. The time delay is $\tau_{n,p}=\tau_n(\boldsymbol{\theta}_p)=2\left\|\boldsymbol{x}_n-\boldsymbol{\theta}_p\right\|/c$, where c is the speed of light, and $f_{n,p}$ denotes the observed Doppler shift, i.e.,

$$f_{n,p} = f_n(\boldsymbol{\theta}_p,\boldsymbol{v}_p) = \frac{2\left(\boldsymbol{x}_n-\boldsymbol{\theta}_p\right)^\top\boldsymbol{v}_p}{c/f_c\left\|\boldsymbol{x}_n-\boldsymbol{\theta}_p\right\|} \tag{5}$$

where f_c is the carrier frequency. We assume there are no targets falling into the same delay and Doppler resolution bins at each local station, i.e.,

$$\min_{\substack{(p,q)\in\{1,\ldots,P\}^2\\ p\neq q}}\min_{n\in\{1,\ldots,N\}}\left|\tau_n(\boldsymbol{\theta}_p)-\tau_n(\boldsymbol{\theta}_q)\right| > \frac{1}{B}, \tag{6}$$

and

$$\min_{\substack{(p,q)\in\{1,\ldots,P\}^2\\ p\neq q}}\min_{n\in\{1,\ldots,N\}}\left|f_n(\boldsymbol{\theta}_p,\boldsymbol{v}_p)-f_n(\boldsymbol{\theta}_q,\boldsymbol{v}_q)\right| > \frac{1}{YT_{\text{pri}}}, \tag{7}$$

and this assumption is called *fully-separable* in this work.

In the following, we sample the received y-th signal $r_{n,y}(t), y=1,...,Y$ in (4) by a sampling interval T_s, thus

[1]Same with [46], this amounts to requiring that each radiated waveform has a thumb-tack auto-correlation function. It should be noted that perfectly orthogonal waveforms may not be feasible solely through waveform design techniques. We aim to obtain closed-form mathematical results, and possible localization performance degradation due to the nonnegligible sidelobes is expected but will not be investigated in this work.

obtaining $M = \lceil T_{\text{pri}}/T_s \rceil$ samples in one PRI, which yields

$$\mathbf{r}_{n,y} = \sum_{p=1}^{P} \alpha_{n,p} d_{n,p,y} \mathbf{s}_{n,p} + \mathbf{w}_{n,y}, \tag{8}$$

where $d_{n,p,y} = e^{\jmath 2\pi f_{n,p}(y-1)T_{\text{pri}}}$,

$$\mathbf{r}_{n,y} = [r_{n,y}(T_s), \ldots, r_{n,y}(MT_s)]^\top \in \mathbb{C}^M, \tag{9}$$

$$\mathbf{s}_{n,p} = [\overline{s}_n(T_s - \tau_{n,p}), \ldots, \overline{s}_n(MT_s - \tau_{n,p})]^\top \in \mathbb{C}^M, \tag{10}$$

$$\mathbf{w}_{n,y} = [w_{n,y}(T_s), \ldots, w_{n,y}(MT_s)]^\top \in \mathbb{C}^M, \tag{11}$$

and $\mathbf{w}_{n,y}[m] \sim \mathcal{CN}(0, \sigma_w^2)$, $m = 1, \ldots, M$.

C. Reassembling of Received Signals

Finally, we reassemble the discrete signals $\{\mathbf{r}_{n,y}\}_{y=1}^{Y}$ in a CPI together to construct a new vector, we have

$$\mathbf{r}_n = \sum_{p=1}^{P} \alpha_{n,p} \mathbf{d}_{n,p} \otimes \mathbf{s}_{n,p} + \mathbf{w}_n, \tag{12}$$

where

$$\mathbf{r}_n = \left[\mathbf{r}_{n,1}^\top \ \ldots \ \mathbf{r}_{n,y}^\top \ \ldots \ \mathbf{r}_{n,Y}^\top\right]^\top \in \mathbb{C}^{MY}, \tag{13}$$

$$\mathbf{w}_n = \left[\mathbf{w}_{n,1}^\top \ \ldots \ \mathbf{w}_{n,y}^\top \ \ldots \ \mathbf{w}_{n,Y}^\top\right]^\top \in \mathbb{C}^{MY}, \tag{14}$$

and

$$\mathbf{d}_{n,p} = \left[1, \ldots, e^{\jmath 2\pi f_{n,p}(y-1)T_{\text{pri}}}, \ldots, e^{\jmath 2\pi f_{n,p}(Y-1)T_{\text{pri}}}\right]^\top \in \mathbb{C}^Y. \tag{15}$$

It should be noted that $\mathbf{d}_{n,p} = \mathbf{d}_n(\boldsymbol{\theta}_p, \boldsymbol{v}_p)$, $\mathbf{s}_{n,p} = \mathbf{s}_n(\boldsymbol{\theta}_p)$, and $\mathbf{w}_n$ is assumed to be a complex circularly-symmetric Gaussian vector with a known diagonal covariance matrix $\mathbf{C}_n = \sigma_w^2 \mathbf{I}_{MY} \in \mathbb{C}^{MY \times MY}$. This assumption is particularly suitable for homogeneous environments like air-search mode. In practical implements, the unknown noise covariance matrix can be estimated using secondary data [35], [55].

III. Joint Detection and Localization of Multiple Moving Targets

In this section, we formulate the JDL of unknown number multiple moving targets problem in a distributed radar system. The goal is to detect the existing unknown number of multiple moving targets and estimate their locations and velocities in location and velocity regions under inspection at the FC, relying on the radar geometry, the transmitted waveforms, and the raw measurements $\mathbf{r}_n$ transmitted from each local station.

A. Problem Formulation

Corresponding to (12), a composite multiple hypothesis testing problem can be formulated, namely,

$$\begin{cases} \mathcal{H}_0: & \mathbf{r}_n = \mathbf{w}_n, \ \forall\, n \\ \mathcal{H}_1: & \mathbf{r}_n = \alpha_{n,1}\mathbf{d}_{n,1} \otimes \mathbf{s}_{n,1} + \mathbf{w}_n, \ \forall\, n \\ & \vdots \\ \mathcal{H}_{P_{\max}}: & \mathbf{r}_n = \sum_{p=1}^{P_{\max}} \alpha_{n,p}\mathbf{d}_{n,p} \otimes \mathbf{s}_{n,p} + \mathbf{w}_n, \ \forall\, n, \end{cases} \tag{16}$$

where $\mathcal{H}_0$ is the null hypothesis, $\mathcal{H}_P$ is the hypothesis that P targets are present at the unknown locations $\boldsymbol{\theta}_1, \ldots, \boldsymbol{\theta}_P$ with unknown gain vectors $\boldsymbol{\alpha}_{n,1:P} = [\alpha_{n,1}, \ldots, \alpha_{n,P}]^\top$, for $n = 1, \ldots, N$, $P = 1, \ldots, P_{\max}$, and the value of $P_{\max} \geq 1$ serves as an upper bound on the number of potential targets. In line with convention, we consider the locations and velocities of the prospective targets to be situated on discrete grids $\mathcal{G}$ and $\mathcal{R}$ in location and velocity regions under inspection, respectively. These grids consist of uniformly spaced points with an inter-element location spacing $\Delta_{\mathcal{G}} \leq c/2B$ and velocity spacing $\Delta_{\mathcal{R}} \leq c/(2f_c Y T_{\text{pri}})$ within the examined location and velocity area, denoted as $\boldsymbol{\theta}_p \in \mathcal{G}$ and $\boldsymbol{v}_p \in \mathcal{R}$, $p = 1, \ldots, P$.

Then, the negative log-likelihood functions of different hypotheses can be written as follows. Under $\mathcal{H}_0$, we have

$$-\ln f_{n,0}(\mathbf{r}_n) = \ln\left(\pi^{MY} \det \mathbf{C}_n\right) + \left\|\mathbf{C}_n^{-1/2}\mathbf{r}_n\right\|^2. \tag{17}$$

Under $\mathcal{H}_P$, for $P = 1, \ldots, P_{\max}$, we have

$$-\ln f_{n,P}(\mathbf{r}_n; \boldsymbol{\theta}_{1:P}, \boldsymbol{v}_{1:P}, \boldsymbol{\alpha}_{n,1:P}) = \ln\left(\pi^{MY} \det \mathbf{C}_n\right) + \left\|\mathbf{C}_n^{-1/2}\left(\mathbf{r}_n - \boldsymbol{\Sigma}_n(\boldsymbol{\theta}_{1:P}, \boldsymbol{v}_{1:P})\boldsymbol{\alpha}_{n,1:P}\right)\right\|^2 \tag{18}$$

where

$$\boldsymbol{\Sigma}_n(\boldsymbol{\theta}_{1:P}, \boldsymbol{v}_{1:P}) = \left[\mathbf{d}_{n,1} \otimes \mathbf{s}_{n,1} \ \ldots \ \mathbf{d}_{n,P} \otimes \mathbf{s}_{n,P}\right] \in \mathbb{C}^{MY \times P} \tag{19}$$

represents the mode matrix comprising the signatures of the targets,

$$\boldsymbol{\alpha}_{n,1:P} = \left[\alpha_{n,1}, \ldots, \alpha_{n,P}\right]^\top \in \mathbb{C}^P \tag{20}$$

is the gain vector, $\boldsymbol{\theta}_{1:P}$ and $\boldsymbol{v}_{1:P}$ are the vectors specifying the locations and velocities of the targets, i.e.,

$$\boldsymbol{\theta}_{1:P} = \text{cat}\{\boldsymbol{\theta}_1, \ldots, \boldsymbol{\theta}_P\} \in \mathcal{G}_{1:P}, \tag{21}$$

and

$$\boldsymbol{v}_{1:P} = \text{cat}\{\boldsymbol{v}_1, \ldots, \boldsymbol{v}_P\} \in \mathcal{R}_{1:P}, \tag{22}$$

respectively, where

$$\mathcal{G}_{1:P} = \Big\{\text{cat}\{\boldsymbol{\theta}_1, \ldots, \boldsymbol{\theta}_P\} \in \mathcal{G}^P : \min_{\substack{(p,q)\in\{1,\ldots,P\}^2 \\ p\neq q}} \min_{n\in\{1,\ldots,N\}} \left|\tau_n(\boldsymbol{\theta}_p) - \tau_n(\boldsymbol{\theta}_q)\right| > 1/B\Big\} \tag{23}$$

and

$$\mathcal{R}_{1:P} = \Big\{\text{cat}\{\boldsymbol{v}_1, \ldots, \boldsymbol{v}_P\} \in \mathcal{R}^P : \min_{\substack{(p,q)\in\{1,\ldots,P\}^2 \\ p\neq q}} \min_{n\in\{1,\ldots,N\}} \left|f_n(\boldsymbol{\theta}_p, \boldsymbol{v}_p) - f_n(\boldsymbol{\theta}_q, \boldsymbol{v}_q)\right| > \frac{1}{YT_{\text{pri}}}\Big\} \tag{24}$$

are the sets specifying all possible positions and velocities of the moving targets.

B. GIC-based Detection and Estimation

At the FC, here we derive a GIC-based detector [56], [57] to solve the JDL problem. An estimate of the number of targets, denoted as $\hat{P}$, can be obtained as

$$\hat{P} = \underset{P\in\{0,\ldots,P_{\max}\}}{\arg\max}\ \mathrm{GIC}(P) \tag{25}$$

where

$$\mathrm{GIC}(P) = \begin{cases} \sum_{n=1}^{N} \ln f_{n,0}\left(\mathbf{r}_n\right), & P=0 \\ \max\limits_{\boldsymbol{\theta}_{1:P}\in\mathcal{G}_{1:P},\boldsymbol{v}_{1:P}\in\mathcal{R}_{1:P}} \sum_{n=1}^{N} \mathcal{F}(\boldsymbol{\theta}_{1:P},\boldsymbol{v}_{1:P},\hat{\boldsymbol{\alpha}}_{n,1:P}) \\ \qquad -\eta NP, \quad P\geq 1, \end{cases} \tag{26}$$

where

$$\mathcal{F}(\boldsymbol{\theta}_{1:P},\boldsymbol{v}_{1:P},\hat{\boldsymbol{\alpha}}_{n,1:P}) = \ln\frac{f_{n,P}\left(\mathbf{r}_n;\boldsymbol{\theta}_{1:P},\boldsymbol{v}_{1:P},\hat{\boldsymbol{\alpha}}_{n,1:P}\right)}{f_{n,0}\left(\mathbf{r}_n\right)} \tag{27}$$

is the LLR function, $\hat{\boldsymbol{\alpha}}_{n,1:P}(\boldsymbol{\theta}_{1:P},\boldsymbol{v}_{1:P})$ is the MLE of the gain vector when the prospective targets are located in $\boldsymbol{\theta}_{1:P}$ with velocities $\boldsymbol{v}_{1:P}$; the penalty factor η is set to have a given probability of false alarm $\mathrm{P_{fa}} = \Pr(\text{reject } \mathcal{H}_0|\mathcal{H}_0)$. Notice that $\hat{\boldsymbol{\alpha}}_{n,1:P}(\boldsymbol{\theta}_{1:P},\boldsymbol{v}_{1:P})$ is available in closed-form, i.e.,

$$\begin{aligned} &\hat{\boldsymbol{\alpha}}_{n,1:P}(\boldsymbol{\theta}_{1:P},\boldsymbol{v}_{1:P}) \\ &= \underset{\boldsymbol{\alpha}_{n,1:P}\in\mathbb{C}^P}{\arg\min} \left\|\mathbf{C}_n^{-1/2}\Big(\mathbf{r}_n - \boldsymbol{\Sigma}_n(\boldsymbol{\theta}_{1:P},\boldsymbol{v}_{1:P})\boldsymbol{\alpha}_{n,1:P}\Big)\right\|^2 \\ &= \Big(\mathbf{C}_n^{-1/2}\boldsymbol{\Sigma}_n(\boldsymbol{\theta}_{1:P},\boldsymbol{v}_{1:P})\Big)^{+}\mathbf{C}_n^{-1/2}\mathbf{r}_n. \end{aligned} \tag{28}$$

Therefore, by substituting (28) into (25) and disregarding irrelevant constant terms, the decision rule based on GIC can be reformulated as

$$\hat{P} = \underset{P\in\{0,\ldots,P_{\max}\}}{\arg\max}\ J(P) \tag{29}$$

where

$$J(P) = \max_{\boldsymbol{\theta}_{1:P}\in\mathcal{G}_{1:P},\boldsymbol{v}_{1:P}\in\mathcal{R}_{1:P}} \sum_{n=1}^{N}\left(\left\|\boldsymbol{\Pi}_n(\boldsymbol{\theta}_{1:P},\boldsymbol{v}_{1:P})\mathbf{C}_n^{-1/2}\mathbf{r}_n\right\|^2\right) - \eta NP \tag{30}$$

for $P\geq 1$, $J(0)=0$, and

$$\boldsymbol{\Pi}_n(\boldsymbol{\theta}_{1:P},\boldsymbol{v}_{1:P}) = \mathbf{C}_n^{-1/2}\boldsymbol{\Sigma}_n(\boldsymbol{\theta}_{1:P},\boldsymbol{v}_{1:P})\Big(\mathbf{C}_n^{-1/2}\boldsymbol{\Sigma}_n(\boldsymbol{\theta}_{1:P},\boldsymbol{v}_{1:P})\Big)^{+}. \tag{31}$$

It is important to emphasize that the scoring metric in (30) incorporates the penalized energies computed independently by each local station, considering the candidate target signatures indexed by $\boldsymbol{\theta}_{1:P}$ and $\boldsymbol{v}_{1:P}$. Then, it compares the maximum over $\mathcal{G}_{1:P}$ and $\mathcal{R}_{1:P}$ with a preset threshold; the arguments of the maximum $\hat{\boldsymbol{\theta}}_{1:P} = \mathrm{cat}\{\hat{\boldsymbol{\theta}}_1,\ldots,\hat{\boldsymbol{\theta}}_P\}$ and $\hat{\boldsymbol{v}}_{1:P} = \mathrm{cat}\{\hat{\boldsymbol{v}}_1,\ldots,\hat{\boldsymbol{v}}_P\}$ are the estimated locations and velocities of targets under $\mathcal{H}_P$. Eventually, the rule in (29) determines the detection decision regarding the number of targets $\hat{P}$, simultaneously the relative estimates $\hat{\boldsymbol{\theta}}_{1:\hat{P}}$ and $\hat{\boldsymbol{v}}_{1:\hat{P}}$ are output. Thus the JDL of multiple moving targets was theoretically implemented.

Remark 1: In practice, this approach is computationally prohibitive. From (30), we can see there is no closed-form solution for $\boldsymbol{\theta}_{1:P}$ and $\boldsymbol{v}_{1:P}$. Instead, we need to employ numerical methods: we assume there are $Q_{\mathcal{G}}$ and $Q_{\mathcal{R}}$ grids in $\mathcal{G}$ and $\mathcal{R}$, respectively, then we should make an enormous search of $(Q_{\mathcal{G}}Q_{\mathcal{R}})^P$ grid points for each assumed P ($P=1,\ldots,P_{\max}$). Therefore, the overall complexity grows exponentially with the number of targets P, surpassing the capabilities of current computing resources.

Remark 2: The computation of $J(P)$ in (30) involves a search over the sets $\mathcal{G}_{1:P}$ and $\mathcal{R}_{1:P}$ whose cardinality scales exponentially with P. More specifically, assume that the whitened mode matrix $\mathbf{C}_n^{-1/2}\boldsymbol{\Sigma}_n(\boldsymbol{\theta}_{1:P},\boldsymbol{v}_{1:P})$ and the whitened measurement $\mathbf{C}_n^{-1/2}\mathbf{r}_n$ is precomputed and stored into a dedicated memory for any grid point $\boldsymbol{\theta}\in\mathcal{G},\boldsymbol{v}\in\mathcal{R}$ and $n=1,\ldots,N$. Then, the computation of the $\boldsymbol{\Pi}_n(\boldsymbol{\theta}_{1:P},\boldsymbol{v}_{1:P})$ requires a pseudoinverse, which costs at most $\mathcal{O}\left(MYP^2\right)$ floating point operations (flops), and a matrix multiplication, which costs $\mathcal{O}\left(M^2Y^2P\right)$ flops; also, the computation of $\left\|\boldsymbol{\Pi}_n(\boldsymbol{\theta}_{1:P},\boldsymbol{v}_{1:P})\mathbf{C}_n^{-1/2}\mathbf{r}_n\right\|^2$ costs $\mathcal{O}\left(M^2Y^2\right)$ flops. Hence, the total cost for computing (30) is at most $\mathcal{O}\big((M^2Y^2P + MYP^2)N(Q_{\mathcal{G}}Q_{\mathcal{R}})^P\big)$ flops.

IV. The Proposed Low-Complexity Solution

In this section, a low-complexity solution is proposed to solve the previously formulated JDL of multiple moving targets problem. Firstly, a problem decomposition is made to partition the joint maximization task of $(Q_{\mathcal{G}}Q_{\mathcal{R}})^P$ grids into P separate optimization problems of $(Q_{\mathcal{G}}Q_{\mathcal{R}})$ grids. Then, we illustrate how to generate the delay- and Doppler-dimensional LLR data which will be transmitted from each radar to the FC for global fusion in practical implementation[2]. Finally, an extended SIC algorithm is devised to extract multiple targets and estimate their locations/velocities step by step.

A. Problem Decomposition

Proposition 1: Following the approximately orthogonality and the *fully-separable* targets assumptions in (3), (4), (6), and (7), (28) can be simplified as

$$\hat{\alpha}_{n,p}(\boldsymbol{\theta}_p,\boldsymbol{v}_p) = \Big(\mathbf{C}_n^{-1/2}(\mathbf{d}_{n,p}\otimes\mathbf{s}_{n,p})\Big)^{+}\mathbf{C}_n^{-1/2}\mathbf{r}_n. \tag{32}$$

The proof of Proposition 1 is given in the Appendix I.

Upon plugging (32) into (25), we can obtain the new

[2]It's worth noting that the GIC-based detector necessitates local stations to transmit raw echoes data $\mathbf{r}_n$, whereas the proposed solution involves transmitting LLR data instead. Although the data transmitting costs remain constant, the proposed solution enables local stations to undertake a portion of the calculations.

expression of the GIC-based rule as

$$\begin{aligned}\{\hat{\boldsymbol{\theta}}_{1:P}, \hat{\boldsymbol{v}}_{1:P}\} &= \underset{\boldsymbol{\theta}_{1:P}\in\mathcal{G}_{1:P}, \boldsymbol{v}_{1:P}\in\mathcal{R}_{1:P}}{\arg\max} \sum_{n=1}^{N}\sum_{p=1}^{P} \ell_n(\boldsymbol{\theta}_p, \boldsymbol{v}_p) - \eta NP \\ &= \underset{\boldsymbol{\theta}_{1:P}\in\mathcal{G}_{1:P}, \boldsymbol{v}_{1:P}\in\mathcal{R}_{1:P}}{\arg\max} \sum_{p=1}^{P} \mathcal{T}\left(\boldsymbol{\theta}_p, \boldsymbol{v}_p\right) - \eta NP,\end{aligned} \tag{33}$$

subject to the targets are *fully-separable*, i.e., the target locations $\boldsymbol{\theta}_{1:P} \in \mathcal{G}_{1:P}$ and velocities $\boldsymbol{v}_{1:P} \in \mathcal{R}_{1:P}$ follow the relationships presented in (6), (7), (23), and (24). Then,

$$\mathcal{T}\left(\boldsymbol{\theta}_p, \boldsymbol{v}_p\right) = \sum_{n=1}^{N} \ell_n(\boldsymbol{\theta}_p, \boldsymbol{v}_p) \tag{34}$$

and

$$\begin{aligned}\ell_n(\boldsymbol{\theta}_p, \boldsymbol{v}_p) = \Big\| &\mathbf{C}_n^{-1/2}(\mathbf{d}_{n,p} \otimes \mathbf{s}_{n,p}) \\ &\left(\mathbf{C}_n^{-1/2}(\mathbf{d}_{n,p} \otimes \mathbf{s}_{n,p})\right)^{+} \mathbf{C}_n^{-1/2}\mathbf{r}_n\Big\|^2\end{aligned} \tag{35}$$

are the objective LLR functions of the p-th target location and velocity, i.e., $\boldsymbol{\theta}_p$ and $\boldsymbol{v}_p$, regarding all stations and the n-th station, respectively.

In practical implementation, the parameters of targets (number, amplitudes, locations, velocities) are unknown and we need to extract them from the objective LLR function regarding N stations and all points within the inspected location and velocity regions $\mathcal{G}$ and $\mathcal{R}$, i.e.,

$$\begin{aligned}\mathcal{T}\left(\boldsymbol{\theta}, \boldsymbol{v}\right) = \sum_{n=1}^{N} \ell_n(\boldsymbol{\theta}, \boldsymbol{v}) = \sum_{n=1}^{N} \Big\| &\mathbf{C}_n^{-1/2}(\mathbf{d}_n\left(\boldsymbol{\theta}, \boldsymbol{v}\right) \otimes \mathbf{s}_n\left(\boldsymbol{\theta}\right)) \\ &\left(\mathbf{C}_n^{-1/2}(\mathbf{d}_n\left(\boldsymbol{\theta}, \boldsymbol{v}\right) \otimes \mathbf{s}_n\left(\boldsymbol{\theta}\right))\right)^{+} \mathbf{C}_n^{-1/2}\mathbf{r}_n\Big\|^2, \boldsymbol{\theta} \in \mathcal{G}, \boldsymbol{v} \in \mathcal{R}.\end{aligned} \tag{36}$$

Because of the *fully-separable* assumption, where no targets are assumed to fall into the same resolution bin of any stations, an effective way to circumvent extensive searching is to determine the maximum of LLR associated with each target regarding all stations while mitigating LLR data from other targets (since $\mathbf{r}_n$ contains the signals of P targets). Hence, the joint maximization task of $(Q_{\mathcal{G}}Q_{\mathcal{R}})^P$ grids will be decomposed into P separate optimization problems of $(Q_{\mathcal{G}}Q_{\mathcal{R}})$ grids, i.e.,

$$\begin{aligned}&\{\hat{\boldsymbol{\theta}}_{1:P}, \hat{\boldsymbol{v}}_{1:P}\} \\ \text{with} \quad &\{\hat{\boldsymbol{\theta}}_p, \hat{\boldsymbol{v}}_p\} = \underset{\boldsymbol{\theta}\in\mathcal{G}, \boldsymbol{v}\in\mathcal{R}}{\arg\max}\ \mathcal{T}_p\left(\boldsymbol{\theta}, \boldsymbol{v}\right) - \eta' N,\end{aligned} \tag{37}$$

where $\mathcal{T}_p\left(\boldsymbol{\theta}, \boldsymbol{v}\right)$ represents the updated function specific to the p-th target and η' is a new penalty factor. This updated function will be further elucidated in the proposed extended SIC algorithm. Before generating the updated function $\mathcal{T}_p\left(\boldsymbol{\theta}, \boldsymbol{v}\right)$ at the FC, we will calculate the practical LLR data matrices at each station, which are shown in Section IV-B.

B. Practical LLR-data Generation

For local radars to undertake a portion of the calculations, the LLR data $\ell_n(\boldsymbol{\theta}, \boldsymbol{v})$ of the n-th local station can be practically calculated in a standardized and discrete manner, without considering $\boldsymbol{\theta}$ and $\boldsymbol{v}$. We denote this data matrix as $\mathbf{L}_n \in \mathbb{C}^{M\times Y}$, i.e.,

$$\mathbf{L}_n = \begin{bmatrix} L_n[1,1] & \cdots & L_n[1,y'] & \cdots & L_n[1,Y] \\ \vdots & \ddots & \vdots & \ddots & \vdots \\ L_n[m',1] & \cdots & L_n[m',y'] & \cdots & L_n[m',Y] \\ \vdots & \ddots & \vdots & \ddots & \vdots \\ L_n[M,1] & \cdots & L_n[M,y'] & \cdots & L_n[M,Y] \end{bmatrix}, \tag{38}$$

where $m' = 1, 2, ..., M$, $y' = 1, 2, ..., Y$, and

$$\begin{aligned}L_n[m',y'] &= \ell_n\left(\boldsymbol{\theta}, \boldsymbol{v} \mid \tau_n^{m'}, f_n^{y'}\right) \\ &= \Big\|\mathbf{C}_n^{-1/2}(\mathbf{d}_n(f_n^{y'}) \otimes \mathbf{s}_n(\tau_n^{m'})) \\ &\quad \left(\mathbf{C}_n^{-1/2}(\mathbf{d}_n(f_n^{y'}) \otimes \mathbf{s}_n(\tau_n^{m'}))\right)^{+} \mathbf{C}_n^{-1/2}\mathbf{r}_n\Big\|^2.\end{aligned} \tag{39}$$

It should be noted that the value of $\tau_n^{m'}$ and $f_n^{y'}$ is discrete, i.e., $\tau_n^{m'} = m'T_s$ and $f_n^{y'} = y'/(T_{\text{pri}}Y)$. In the calculation of each element of L_n, e.g., $L_n[m',y']$, we directly substitute the corresponding $\tau_n^{m'}$ and $f_n^{y'}$ to $\mathbf{s}_n$ and $\mathbf{d}_n$ in (10) and (15), respectively. Then a delay- and Doppler-dimensional LLR data matrix will be generated at each local station and is assumed to be completely transmitted to the FC for global data fusion.

Remark 3: The complete transmission of the LLR data matrix will impose a large load, as all matrix elements need to be quantized and transmitted while maintaining the real-time nature of information processing. For instance, the data matrix obtained from a CPI must be transmitted to the FC within at least the following T_{cpi} period. When the communication bandwidth between each radar and the fusion center is constrained (e.g., using wireless communication links in a communication-constrained environment), this load will become unaffordable, and transmitting complete LLR data will be unrealistic. Current methods, such as low-bit quantization [40] or censoring [58], make it possible to reduce the transmission load. However, this problem is not the focus of this paper and will be explored in our future works.

Hence, in practice, the FC will utilize the received LLR data matrices $\mathbf{L}_n \in \mathbb{C}^{M\times Y}, n = 1, \ldots, N$ to make data fusion. Then, (36) can be rewritten as

$$\begin{aligned}\mathcal{T}\left(\boldsymbol{\theta}, \boldsymbol{v}\right) &= \sum_{n=1}^{N} \ell_n(\boldsymbol{\theta}, \boldsymbol{v}) \\ &= \sum_{n=1}^{N} L_n[\lceil \tau_n(\boldsymbol{\theta})/T_s \rceil, \lceil f_n(\boldsymbol{\theta}, \boldsymbol{v}) T_{\text{pri}} Y \rceil], \boldsymbol{\theta} \in \mathcal{G}, \boldsymbol{v} \in \mathcal{R}.\end{aligned} \tag{40}$$

Remark 4: In (40), the FC receives different LLR data matrices $\mathbf{L}_n \in \mathbb{C}^{M\times Y}, n = 1, \ldots, N$ and proceeds to perform data association. Given that the FC possesses knowledge about the locations of local stations, we traverse different positions and velocities $\boldsymbol{\theta} \in \mathcal{G}, \boldsymbol{v} \in \mathcal{R}$ by calculating $\lceil \tau_n(\boldsymbol{\theta})/T_s \rceil$ and $\lceil f_n(\boldsymbol{\theta}, \boldsymbol{v}) T_{\text{pri}} Y \rceil$ to determine the values in $\mathbf{L}_n \in \mathbb{C}^{M\times Y}, n = 1, \ldots, N$ corresponding to the pair $(\boldsymbol{\theta}, \boldsymbol{v})$. Thus the data association in the FC has been implemented.

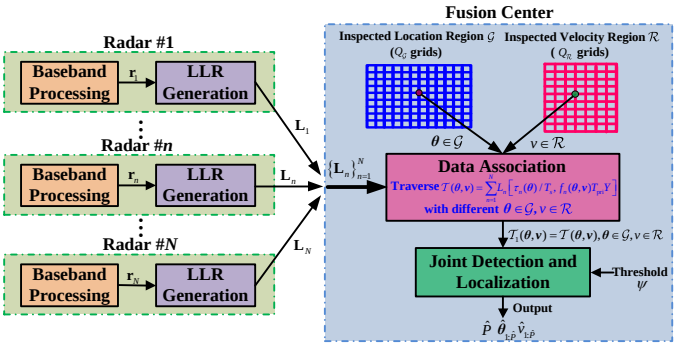

Fig. 2. The structure of the proposed low-complexity solution.

C. Extended SIC Algorithm

At the FC, the challenge we currently face is how to extract the targets from $\mathcal{T}(\boldsymbol{\theta},\boldsymbol{v})$ in (40) while mitigating influences among them, thus realizing high-performance joint detection and localization of every moving target. Leveraging the design methodology of the SIC algorithm proposed in [46], in this subsection we devise an extended SIC algorithm to extract multiple moving targets and estimate their number, locations, and velocities in multiple iterations. Each iteration extracts one and simultaneously output its estimated location $\hat{\boldsymbol{\theta}}_p$ and velocity $\hat{\boldsymbol{v}}_p$, $p=1,\ldots,\hat{P}$, and the estimated target number $\hat{P}$ will be finally determined. For a clearer illustration, the structure of the proposed solution is shown in Fig. 2.

Here we elaborate the devised algorithm by multiple steps:

1) **Step 1**: At the p-th iteration, traverse $\mathcal{T}_p(\boldsymbol{\theta},\boldsymbol{v})$ ($p=1,\ldots,P_{\max}$ and $\mathcal{T}_1(\boldsymbol{\theta},\boldsymbol{v})=\mathcal{T}(\boldsymbol{\theta},\boldsymbol{v})$) with different $\boldsymbol{\theta}\in\mathcal{G}$ and $\boldsymbol{v}\in\mathcal{R}$ at the p-th iteration. One iteration will generate a location data plane including $Q_{\mathcal{G}}$ grids, and each location grid will generate a velocity data plane including $Q_{\mathcal{R}}$ grids (e.g., Fig. 4 in the simulation section);
2) **Step 2**: Find the maximum value of all of the data planes. If it exceeds the preset threshold ψ, the p-th target is declared and the corresponding location $\boldsymbol{\theta}_p$ and velocity $\boldsymbol{v}_p$ will be extracted as its estimations $\{\hat{\boldsymbol{\theta}}_p,\hat{\boldsymbol{v}}_p\}$. Therefore, the detector at the p-th iteration can be computed as

$$\begin{aligned}&\{\hat{\boldsymbol{\theta}}_p,\hat{\boldsymbol{v}}_p\}=\arg\max_{\boldsymbol{\theta}\in\mathcal{G},\boldsymbol{v}\in\mathcal{R}}\mathcal{T}_p(\boldsymbol{\theta},\boldsymbol{v})\\ &\text{s.t.}\quad\max_{\boldsymbol{\theta}\in\mathcal{G},\boldsymbol{v}\in\mathcal{R}}\mathcal{T}_p(\boldsymbol{\theta},\boldsymbol{v})\geq\psi,\ p\leq P_{\max}\end{aligned}\tag{41}$$

where ψ is the detection threshold that can be numerically set[3] given a constant global false alarm probability

$$\mathrm{P_{fa}}=\Pr(\max_{\boldsymbol{\theta}\in\mathcal{G},\boldsymbol{v}\in\mathcal{R}}\mathcal{T}(\boldsymbol{\theta},\boldsymbol{v})>\psi\mid\mathcal{H}_0).\tag{42}$$

[3]In simulations or realistic implements, given a set $\mathrm{P_{fa}}$ and following (42), the threshold ψ can be determined numerically by generating the functions $\mathcal{T}^{(i)}(\boldsymbol{\theta},\boldsymbol{v})$ under the $\mathcal{H}_0$ hypothesis and using target-free noise data for $i=1,\ldots,\lceil z/\mathrm{P_{fa}}\rceil$ independent trials, where z is a set positive integer, $\boldsymbol{\theta}\in\mathcal{G}$, and $\boldsymbol{v}\in\mathcal{R}$. The noise data at each trial are randomly generated or recorded in target-free realistic scenarios. Then the maximum values $\hat{\psi}^{(i)}=\max_{\boldsymbol{\theta}\in\mathcal{G},\boldsymbol{v}\in\mathcal{R}}\mathcal{T}^{(i)}(\boldsymbol{\theta},\boldsymbol{v})$ will be extracted for each trial and sorted in descending order to form a vector $\mathbf{F}\in\mathbb{C}^{\lceil z/\mathrm{P_{fa}}\rceil}$. Finally, the detection threshold is output as $\psi=\mathbf{F}[z]$.

Algorithm 1 Implementation of the proposed algorithm

provide Finite grids $\mathcal{G}$ and $\mathcal{R}$ in location and velocity regions under inspection, respectively, detection threshold ψ, the assumed upper bound of the prospective targets number $P_{\max}$, the discrete LLR values $\mathbf{L}_n$ ($n=1,\ldots,N$), and the number of detected targets $\hat{P}=0$.
for $p=1,\ldots,P_{\max}$ **do**
  Compute $\mathcal{T}_p(\boldsymbol{\theta},\boldsymbol{v})$ from (45)
  if $\max_{\boldsymbol{\theta}\in\mathcal{G},\boldsymbol{v}\in\mathcal{R}}\mathcal{T}_p(\boldsymbol{\theta},\boldsymbol{v})\geq\psi$ **then**
    Compute $\{\hat{\boldsymbol{\theta}}_p,\hat{\boldsymbol{v}}_p\}=\arg\max_{\boldsymbol{\theta}\in\mathcal{G},\boldsymbol{v}\in\mathcal{R}}\mathcal{T}_p(\boldsymbol{\theta},\boldsymbol{v})$
    Compute $\hat{P}=\hat{P}+1$
  else
    break
  end if
end for
return The estimated target number $\hat{P}$, locations $\hat{\boldsymbol{\Theta}}_{ML}=\hat{\boldsymbol{\theta}}_{1:\hat{P}}$, and velocities $\hat{\boldsymbol{V}}_{ML}=\hat{\boldsymbol{v}}_{1:\hat{P}}$.

3) **Step 3**: Eliminate the data of the extracted target within a delay and Doppler resolution bin from the p-th LLR matrix $\mathbf{L}_{n,p}$ to obtain a new matrix $\mathbf{L}_{n,p+1}$ ($n=1,\ldots,N,p=1,\ldots,P_{\max}$ and $\mathbf{L}_{n,1}=\mathbf{L}_n$), i.e.,

$$\begin{aligned}&L_{n,p+1}[\lceil\tau_n(\boldsymbol{\theta})/T_s\rceil,\lceil f_n(\boldsymbol{\theta},\boldsymbol{v})T_{\text{pri}}Y\rceil]=\\ &\begin{cases}0,\{\boldsymbol{\theta},\boldsymbol{v}\}\in\mathbb{D}_n\left(\{\boldsymbol{\theta},\boldsymbol{v}\};\{\hat{\boldsymbol{\theta}}_p,\hat{\boldsymbol{v}}_p\}\right)\\ L_{n,p}[\lceil\tau_n(\boldsymbol{\theta})/T_s\rceil,\lceil f_n(\boldsymbol{\theta},\boldsymbol{v})YT_{\text{pri}}\rceil],\text{others},\end{cases}\end{aligned}\tag{43}$$

where

$$\begin{aligned}&\mathbb{D}_n\left(\{\boldsymbol{\theta},\boldsymbol{v}\};\{\hat{\boldsymbol{\theta}}_p,\hat{\boldsymbol{v}}_p\}\right)=\Big\{\{\boldsymbol{\theta},\boldsymbol{v}\}\big|\mid\tau_n(\boldsymbol{\theta})-\tau_n(\hat{\boldsymbol{\theta}}_p)\mid\\ &\leq\frac{1}{B},\mid f_n(\boldsymbol{\theta},\boldsymbol{v})-f_n(\hat{\boldsymbol{\theta}}_p,\hat{\boldsymbol{v}}_p)\mid\leq\frac{1}{YT_{\text{pri}}},\boldsymbol{\theta}\in\mathcal{G},\boldsymbol{v}\in\mathcal{R}\Big\}.\end{aligned}\tag{44}$$

Then we can obtain a new objective LLR function

$$\mathcal{T}_{p+1}(\boldsymbol{\theta},\boldsymbol{v})=\sum_{n=1}^{N}L_{n,p+1}[\lceil\tau_n(\boldsymbol{\theta})/T_s\rceil,\lceil f_n(\boldsymbol{\theta},\boldsymbol{v})T_{\text{pri}}Y\rceil]\tag{45}$$

for the $(p+1)$-th iteration;
4) **Step 4**: Repeat the previous steps until the maximum value of the updated objective LLR function cannot exceed the threshold or $p>P_{\max}$. Finally, output the estimated target number $\hat{P}=p-1$ and all estimated locations $\hat{\boldsymbol{\Theta}}_{ML}=\hat{\boldsymbol{\theta}}_{1:\hat{P}}$ and velocities $\hat{\boldsymbol{V}}_{ML}=\hat{\boldsymbol{v}}_{1:\hat{P}}$.

To summarize, the proposed extended SIC algorithm operates iteratively, with each iteration focusing on the detection and localization of one target. When a target is extracted and its location and velocity are estimated by maximizing its LLR function in (41), the LLR data matrix and the LLR function will be updated by (43)–(45) to clear the LLR data of this target and prepare for the next iteration. The overall procedure is summarized in Algorithm 1.

Remark 5: From the previous summary of the extended SIC algorithm, it can be seen that the primary factor driving the computational expenses is the computation of the objective

TABLE I
SIMULATION PARAMETERS

Parameter	Value
Number of Radars, N	3
Carrier Frequency, f_c	10 GHz
Bandwidth, B	5 MHz
Sampling Interval, T_s	0.1 us
PRI, T_{pri}	75 us
Samples in a PRI, M	750
The Number of PRIs in a CPI, Y	256
CPI, T_{cpi}	19.2 ms
Range Bin, $cT_s/2$	15 m
Noise Variance, σ_w^2	1
Global False Alarm Probability, P_{fa}	2.5×10^{-3}

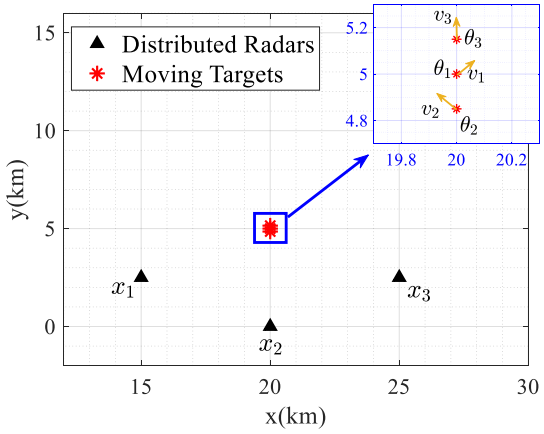

Fig. 3. The 18 km × 18 km plane which involves three distributed radars and three moving targets.

LLR function $\mathcal{T}(\boldsymbol{\theta}, \boldsymbol{v})$ in (40). For a specific sample point in the LLR data matrix $\mathbf{L}_n \in \mathbb{C}^{M\times Y}$ of (38), its computational load is bounded by $\mathcal{O}\left(M^2Y^2+MY\right)$ flops. Then, for the total MY points and N stations, its computational load is bounded by $\mathcal{O}\left(NM^3Y^3\right)$ flops. At the FC, since there are $Q_{\mathcal{G}}$ and $Q_{\mathcal{R}}$ grids in the inspected location and velocity regions $\mathcal{G}$ and $\mathcal{R}$, the cost for computing the $\mathcal{T}(\boldsymbol{\theta}, \boldsymbol{v})$ regarding all stations and all inspected grids is $\mathcal{O}\left(NQ_{\mathcal{G}}Q_{\mathcal{R}}\right)$ flops. Besides, the updating of the new objective LLR function at each iteration costs $\mathcal{O}\left(NQ_{\mathcal{G}}Q_{\mathcal{R}}\right)$ flops. Finally, considering there are P times of potential loops, the total costs for computing the extended SIC algorithm is at least $\mathcal{O}\left(NM^3Y^3 + PNQ_{\mathcal{G}}Q_{\mathcal{R}}\right)$ flops.

V. NUMERICAL RESULTS

In this section, we illustrate the effectiveness of the proposed algorithm by considering a distributed radar system, comprised of three radars, monitoring three targets. The parameters and geometry of the radars and moving targets are shown in Table I and Fig. 3, respectively. The radars are placed at $\boldsymbol{x}_1 = (15, 2.5)$ km, $\boldsymbol{x}_2 = (20, 0)$ km, and $\boldsymbol{x}_3 = (25, 2.5)$ km. The targets are placed at $\boldsymbol{\theta}_1 = (20, 5)$ km, $\boldsymbol{\theta}_2 = (20, 4.85)$ km, and $\boldsymbol{\theta}_3 = (20, 5.15)$ km with velocities $\boldsymbol{v}_1 = (6, 6)$ m/s, $\boldsymbol{v}_2 = (-7, 4)$ m/s, and $\boldsymbol{v}_3 = (0, 7)$ m/s, respectively. The ratio of the modulus of the complex amplitudes between different targets is given by $|\alpha_{n,1}| : |\alpha_{n,2}| : |\alpha_{n,3}| = 1 : 0.8 : 0.6$. We use $\lceil 100/\text{P}_{\text{fa}} \rceil$ and 3000 Monte Carlo (MC) trials to set the detection threshold and obtain the performance results, respectively. All results were obtained using MATLAB 2021a on a machine with 256 GB of memory and two 2.5 GHz Intel Xeon E5-2678V3 CPUs, each containing 12 cores and 24 threads. Besides, the probability of target detection (P_{d}) and the root mean square error (RMSE) of estimation serve as metrics for evaluating the performance of detection, localization, and velocity estimation. In particular, under $\bar{\mathcal{H}}_0$, we say that Target q ($q = 1, \ldots, P$ and $P = 3$) is detected if the event $\tilde{E}_q = \{ \min_{p\in\{1,\ldots,\hat{P}\}} \|\hat{\boldsymbol{\theta}}_p - \boldsymbol{\theta}_q\| \leq c/2B\}$ is true. Accordingly, the probability of detecting Target q is

$$\text{P}_{\text{d}} = \Pr\left(\tilde{E}_q | \bar{\mathcal{H}}_0\right). \tag{46}$$

Once the event $\tilde{E}_q$ occurs, the exact estimated location of Target q can be output as

$$\hat{\boldsymbol{\theta}}_q = \underset{\hat{\boldsymbol{\theta}}\in\{\hat{\boldsymbol{\theta}}_1,\ldots,\hat{\boldsymbol{\theta}}_{\hat{P}}\}}{\arg\min} \|\hat{\boldsymbol{\theta}} - \boldsymbol{\theta}_q\|. \tag{47}$$

Then, its corresponding estimated velocity $\hat{\boldsymbol{v}}_q$ will be obtained since the procedure in (41) outputs an estimated location and velocity simultaneously. Therefore, the RMSEs in the estimation of location, velocity, and velocity direction of Target q are calculated by

$$\text{RMSE}_{\text{location}} = \sqrt{\mathbb{E}\left[\|\hat{\boldsymbol{\theta}}_q - \boldsymbol{\theta}_q\|^2 \big| \tilde{E}_q, \bar{\mathcal{H}}_0\right]}, \tag{48}$$

$$\text{RMSE}_{\text{velocity}} = \sqrt{\mathbb{E}\left[(\|\hat{\boldsymbol{v}}_q\| - \|\boldsymbol{v}_q\|)^2 \big| \tilde{E}_q, \bar{\mathcal{H}}_0\right]}, \tag{49}$$

and

$$\text{RMSE}_{\text{direction}} = \sqrt{\mathbb{E}\left[\left(\frac{180^\circ}{\pi} \arccos\left(\frac{\hat{\boldsymbol{v}}_q \cdot \boldsymbol{v}_q}{\|\hat{\boldsymbol{v}}_q\|\|\boldsymbol{v}_q\|}\right)\right)^2 \big| \tilde{E}_q, \bar{\mathcal{H}}_0\right]}, \tag{50}$$

respectively. In the following, two benchmarks are considered for comparison:

(a) The GLRT detector with cleaned data (GLRT-CD) [46], [47], which ideally removes the received echoes of other targets. It should be noted that the GLRT-CD benchmark is equivalent to the computationally-prohibitive GIC-based detector when only one target exists.
(b) The original GLRT detector (O-GLRT), proposed in [43], achieves the highest detection performance for multiple moving targets among the algorithms proposed in that state-of-the-art work.

We first show the output data planes of the proposed algorithm over three iterations in a single trial, which are reported in Fig. 4. It is verified that during the three iterations, the proposed algorithm was able to correctly detect a target each time and simultaneously estimate its corresponding location and velocity. The detection of weaker targets will not be influenced by the strong target since our designed iterative cancellation steps can effectively mitigate the LLR data of the previously detected targets.

Then, the detection performance outcomes of the proposed algorithm and the utilized benchmarks are presented in Fig.

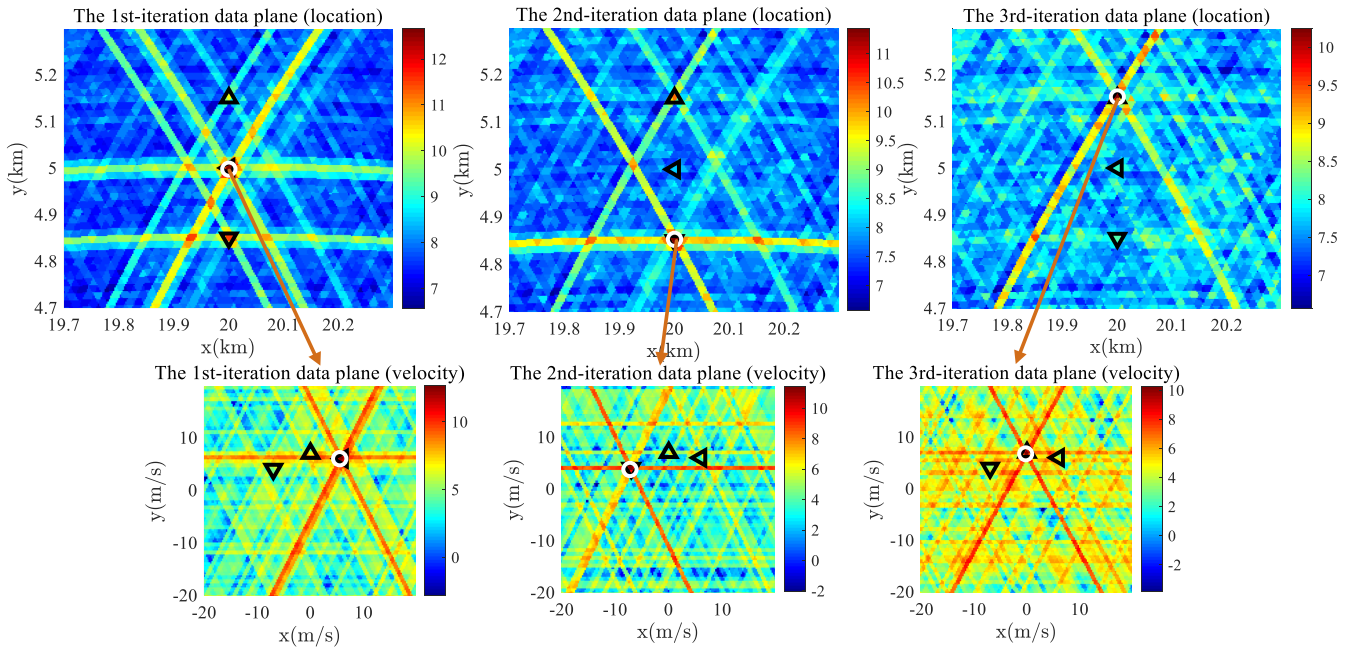

Fig. 4. Output data planes of the proposed algorithm ($\mathcal{T}_{\boldsymbol{p}}(\boldsymbol{\theta}, \boldsymbol{v})$ in (45), $\boldsymbol{p} = 1, 2, 3$: the top three are the location data planes where each value of the location grid is the maximum of its corresponding velocity data plane; the bottom three are the velocity data planes corresponding to the location grid ($\boldsymbol{\theta} = \hat{\boldsymbol{\theta}}_{\boldsymbol{p}}$) in three consecutive iterations when SNR $= 15$ dB. The triangle markers are the true target locations/velocities; the circle marker is the estimated location/velocity of the detected target at each iteration; all estimated results in this single trial closely match the ground truth.

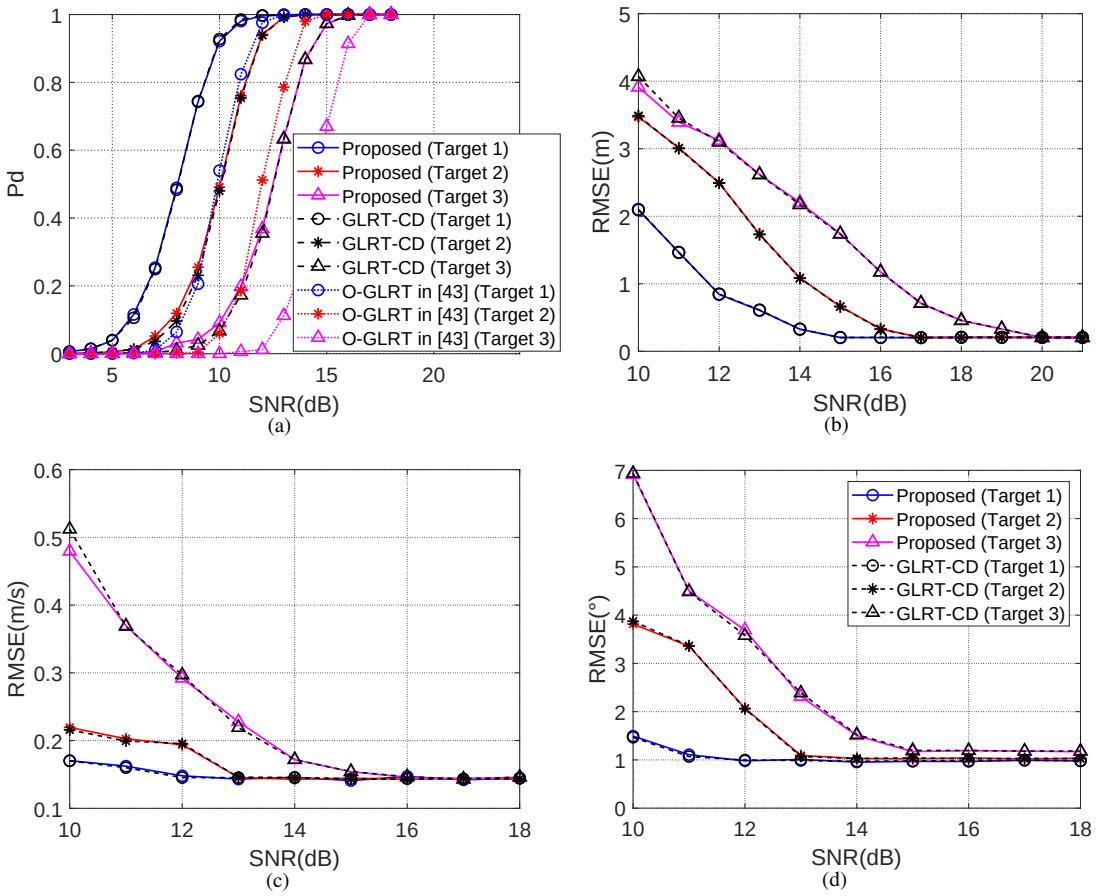

Fig. 5. P_d and RMSE results of all targets versus SNR: (a) P_d; (b) RMSE in the location estimate; (c) RMSE in the velocity estimate; (d) RMSE in the velocity direction estimate.

5(a). It is evident that the detection performance of the proposed algorithm is close to the single-target benchmark GLRT-CD for all targets, which demonstrates the accuracy of target extraction regardless of the influences from other targets. Compared with our proposed solution, the O-GLRT detector performs a detection performance gap because it makes the data fusion of the maximum of the Doppler shifts (as seen in [43, eq. (26)]), which will result in ineffective accumulation of target energy when the noise points are selected, especially in the low-SNR environment.

Finally, we also investigate the RMSEs in the estimates of location, velocity, and velocity direction. Here, we treat the angle between the estimated and the true velocity as the velocity direction metric, as illustrated in (50). These investigations are presented in Figs. 5(b), (c), and (d). From these figures, it is evident that the RMSEs for all estimation metrics of the targets are well within acceptable limits, indicating high accuracy in our estimates. Specifically, the figures show that the proposed algorithm achieves precise localization and velocity estimation, even in challenging scenarios with multiple targets. The consistency and accuracy of these estimations further highlight the robustness and reliability of our approach. Therefore, the effectiveness of the proposed algorithm is clearly demonstrated.

VI. Conclusion

This paper has addressed the JDL of multiple moving targets in a distributed radar system. We first formulated the JDL problem as a composite multiple hypothesis testing problem and derived a GIC-based detector to simultaneously detect the targets and estimate their unknown parameters. However, the overall complexity grows exponentially with the unknown number of targets. Then we proposed a low-complexity algorithm, utilizing the devised several iterative steps to efficiently realize the JDL of multiple moving targets. Finally, comprehensive simulations including three moving targets have been conducted to showcase the effectiveness of the proposed algorithm. Future works may explore distributed radars with partial/no knowledge of the noise covariance matrices; the case of cooperative-communicating targets; and the strategies to attain achievable detection and localization performance of moving targets when the communication bandwidth between each local station and the fusion center is constrained.

Appendix I
Proof of Proposition 1

Given (19) and (20), (28) can be further formulated as

$$\begin{aligned}
&\hat{\boldsymbol{\alpha}}_{n,1:P}(\boldsymbol{\theta}_{1:P}, \boldsymbol{v}_{1:P}) \\
&= \left[\hat{\alpha}_{n,1}(\boldsymbol{\theta}_1, \boldsymbol{v}_1), \ldots, \hat{\alpha}_{n,P}(\boldsymbol{\theta}_P, \boldsymbol{v}_P)\right]^\top \\
&= \left(\mathbf{C}_n^{-1/2}\boldsymbol{\Sigma}_n(\boldsymbol{\theta}_{1:P}, \boldsymbol{v}_{1:P})\right)^+ \mathbf{C}_n^{-1/2}\mathbf{r}_n \\
&= \left(\mathbf{C}_n^{-1/2}\left[\mathbf{d}_{n,1}\otimes\mathbf{s}_{n,1} \ \ldots \ \mathbf{d}_{n,P}\otimes\mathbf{s}_{n,P}\right]\right)^+ \mathbf{C}_n^{-1/2}\mathbf{r}_n \\
&= \left[\mathbf{C}_n^{-1/2}\mathbf{d}_{n,1}\otimes\mathbf{s}_{n,1} \ \ldots \ \mathbf{C}_n^{-1/2}\mathbf{d}_{n,P}\otimes\mathbf{s}_{n,P}\right]^+ \mathbf{C}_n^{-1/2}\mathbf{r}_n \\
&= \mathbf{H}^+\mathbf{C}_n^{-1/2}\mathbf{r}_n \in \mathbb{C}^P,
\end{aligned} \tag{51}$$

where

$$\begin{aligned}
\mathbf{H} &= \left[\mathbf{h}_1 \ \ldots \ \mathbf{h}_P\right] \\
&= \left[\mathbf{C}_n^{-1/2}\mathbf{d}_{n,1}\otimes\mathbf{s}_{n,1} \ \ldots \ \mathbf{C}_n^{-1/2}\mathbf{d}_{n,P}\otimes\mathbf{s}_{n,P}\right] \in \mathbb{C}^{MY\times P}.
\end{aligned} \tag{52}$$

Following the approximately orthogonality in (3) and (4), i.e., the term $\overline{s}_n(t)$ in $\mathbf{s}_n$ has a narrow-pulse property in time domain and the auto-terms $\overline{s}_n(t-\tau_{n,p})$ and $\overline{s}_n(t-\tau_{n,q})$ are orthogonal if $(\tau_{n,p}\neq\tau_{n,q})$ [46, eq. (27) and footnote 4], and the *fully-separable* targets assumptions in (6) and (7), then we can obtain that the P terms $\mathbf{d}_{n,p}\otimes\mathbf{s}_{n,p}, p=1,\ldots,P$ are orthogonal with each other. Since $\mathbf{C}_n = \sigma_w^2\mathbf{I}_{MY} \in \mathbb{C}^{MY\times MY}$, the P terms $\mathbf{h}_p = \mathbf{C}_n^{-1/2}\mathbf{d}_{n,p}\otimes\mathbf{s}_{n,p}, p=1,\ldots,P$ are still orthogonal with each other.

To calculate the expansion of $\mathbf{H}^+$, we first present the following theorem.

Theorem 1: Let $\mathbf{A}$ be an $MY\times P$ matrix with orthogonal column vectors $\mathbf{a}_1, \mathbf{a}_2, \ldots, \mathbf{a}_P$, i.e.,

$$\mathbf{a}_i^\top\mathbf{a}_j = 0 \quad \text{for} \quad i\neq j. \tag{53}$$

Then the pseudoinverse of $\mathbf{A}$ is given by

$$\mathbf{A}^+ = \begin{bmatrix}\mathbf{a}_1^H/\|\mathbf{a}_1\|^2 \\ \mathbf{a}_2^H/\|\mathbf{a}_2\|^2 \\ \cdots \\ \mathbf{a}_P^H/\|\mathbf{a}_P\|^2\end{bmatrix} = \begin{bmatrix}\mathbf{a}_1^+ \\ \mathbf{a}_2^+ \\ \cdots \\ \mathbf{a}_P^+\end{bmatrix}. \tag{54}$$

Proof:

The pseudoinverse of $\mathbf{A}$ is expressed as

$$\mathbf{A}^+ = (\mathbf{A}^H\mathbf{A})^{-1}\mathbf{A}^H. \tag{55}$$

Since the column vectors are orthogonal, the matrix $\mathbf{A}^H\mathbf{A}$ is a diagonal matrix with diagonal elements being the squared norms of each column vector:

$$\mathbf{A}^H\mathbf{A} = \text{diag}(\|\mathbf{a}_1\|^2, \|\mathbf{a}_2\|^2, \ldots, \|\mathbf{a}_P\|^2). \tag{56}$$

Therefore, $(\mathbf{A}^H\mathbf{A})^{-1}$ is also a diagonal matrix which can be represented as

$$(\mathbf{A}^H\mathbf{A})^{-1} = \text{diag}\left(\frac{1}{\|\mathbf{a}_1\|^2}, \frac{1}{\|\mathbf{a}_2\|^2}, \ldots, \frac{1}{\|\mathbf{a}_P\|^2}\right). \tag{57}$$

Consequently, by substituting (57) into (55), $\mathbf{A}^+$ can be written as:

$$\begin{aligned}
\mathbf{A}^+ &= \text{diag}\left(\frac{1}{\|\mathbf{a}_1\|^2}, \frac{1}{\|\mathbf{a}_2\|^2}, \ldots, \frac{1}{\|\mathbf{a}_P\|^2}\right)\mathbf{A}^H \\
&= \begin{bmatrix}\mathbf{a}_1^H/\|\mathbf{a}_1\|^2 \\ \mathbf{a}_2^H/\|\mathbf{a}_2\|^2 \\ \cdots \\ \mathbf{a}_P^H/\|\mathbf{a}_P\|^2\end{bmatrix} = \begin{bmatrix}\mathbf{a}_1^+ \\ \mathbf{a}_2^+ \\ \cdots \\ \mathbf{a}_P^+\end{bmatrix},
\end{aligned} \tag{58}$$

which is the desired form. ■

Following Theorem 1, we can obtain

$$\mathbf{H}^+ = \begin{bmatrix}\mathbf{h}_1^+ \\ \cdots \\ \mathbf{h}_p^+ \\ \cdots \\ \mathbf{h}_P^+\end{bmatrix} = \begin{bmatrix}(\mathbf{C}_n^{-1/2}\mathbf{d}_{n,1}\otimes\mathbf{s}_{n,1})^+ \\ \cdots \\ (\mathbf{C}_n^{-1/2}\mathbf{d}_{n,p}\otimes\mathbf{s}_{n,p})^+ \\ \cdots \\ (\mathbf{C}_n^{-1/2}\mathbf{d}_{n,P}\otimes\mathbf{s}_{n,P})^+\end{bmatrix} \in \mathbb{C}^{P\times MY}. \tag{59}$$

Finally, by substituting (59) into (51), the equation can be rewritten as

$$\begin{bmatrix} \hat{\alpha}_{n,1}(\boldsymbol{\theta}_1, \boldsymbol{v}_1) \\ \cdots \\ \hat{\alpha}_{n,p}(\boldsymbol{\theta}_p, \boldsymbol{v}_p) \\ \cdots \\ \hat{\alpha}_{n,P}(\boldsymbol{\theta}_P, \boldsymbol{v}_P) \end{bmatrix} = \begin{bmatrix} (\mathbf{C}_n^{-1/2}\mathbf{d}_{n,1} \otimes \mathbf{s}_{n,1})^{+}\mathbf{C}_n^{-1/2}\mathbf{r}_n \\ \cdots \\ (\mathbf{C}_n^{-1/2}\mathbf{d}_{n,p} \otimes \mathbf{s}_{n,p})^{+}\mathbf{C}_n^{-1/2}\mathbf{r}_n \\ \cdots \\ (\mathbf{C}_n^{-1/2}\mathbf{d}_{n,P} \otimes \mathbf{s}_{n,P})^{+}\mathbf{C}_n^{-1/2}\mathbf{r}_n \end{bmatrix}. \tag{60}$$

Therefore

$$\hat{\alpha}_{n,p}(\boldsymbol{\theta}_p, \boldsymbol{v}_p) = (\mathbf{C}_n^{-1/2}(\mathbf{d}_{n,p} \otimes \mathbf{s}_{n,p}))^{+}\mathbf{C}_n^{-1/2}\mathbf{r}_n, \tag{61}$$

and Proposition 1 is proved.

REFERENCES

[1] C. Baker and A. Hume, "Netted radar sensing," *IEEE Aerospace and Electronic Systems Magazine*, vol. 18, no. 2, pp. 3–6, 2003.

[2] S. Zhao, L. Zhang, Y. Zhou, and N. Liu, "Signal fusion-based algorithms to discriminate between radar targets and deception jamming in distributed multiple-radar architectures," *IEEE Sensors Journal*, vol. 15, no. 11, pp. 6697–6706, 2015.

[3] C. Shi, L. Ding, F. Wang, S. Salous, and J. Zhou, "Low probability of intercept-based collaborative power and bandwidth allocation strategy for multi-target tracking in distributed radar network system," *IEEE Sensors Journal*, vol. 20, no. 12, pp. 6367–6377, 2020.

[4] J. Yan, H. Liu, W. Pu, B. Jiu, Z. Liu, and Z. Bao, "Benefit analysis of data fusion for target tracking in multiple radar system," *IEEE Sensors Journal*, vol. 16, no. 16, pp. 6359–6366, 2016.

[5] S. Waqar, M. Muaaz, and M. Pätzold, "Direction-independent human activity recognition using a distributed MIMO radar system and deep learning," *IEEE Sensors Journal*, vol. 23, no. 20, pp. 24 916–24 929, 2023.

[6] Y. Kong, S. Xia, L. Dong, X. Yu, and G. Cui, "Compound jamming recognition via contrastive learning for distributed MIMO radars," *IEEE Transactions on Vehicular Technology*, vol. 73, no. 6, pp. 7892–7907, 2024.

[7] X. Liu, Z.-H. Xu, L. Wang, W. Dong, and S. Xiao, "Cognitive dwell time allocation for distributed radar sensor networks tracking via cone programming," *IEEE Sensors Journal*, vol. 20, no. 10, pp. 5092–5101, 2020.

[8] E. Fishler, A. Haimovich, R. S. Blum, L. J. Cimini, D. Chizhik, and R. A. Valenzuela, "Spatial diversity in radars–Models and detection performance," *IEEE Transactions on Signal Processing*, vol. 54, no. 3, pp. 823–838, Feb. 2006.

[9] L. Wang, M. Cheney, and B. Borden, "Multistatic radar imaging of moving targets," *IEEE Transactions on Aerospace and Electronic Systems*, vol. 48, no. 1, pp. 230–242, 2012.

[10] A. M. Haimovich, R. S. Blum, and L. J. Cimini, "MIMO radar with widely separated antennas," *IEEE Signal Processing Magazine*, vol. 25, no. 1, pp. 116–129, Jan. 2007.

[11] S. Gogineni and A. Nehorai, "Polarimetric MIMO radar with distributed antennas for target detection," *IEEE Transactions on Signal Processing*, vol. 58, no. 3, pp. 1689–1697, 2009.

[12] H. Godrich, A. P. Petropulu, and H. V. Poor, "Sensor selection in distributed multiple-radar architectures for localization: A knapsack problem formulation," *IEEE Transactions on Signal Processing*, vol. 60, no. 1, pp. 247–260, 2011.

[13] M. Sadeghi, F. Behnia, R. Amiri, and A. Farina, "Target localization geometry gain in distributed MIMO radar," *IEEE Transactions on Signal Processing*, vol. 69, pp. 1642–1652, 2021.

[14] H. Li, A. Mehul, J. Le Kernec, S. Z. Gurbuz, and F. Fioranelli, "Sequential human gait classification with distributed radar sensor fusion," *IEEE Sensors Journal*, vol. 21, no. 6, pp. 7590–7603, 2020.

[15] J. Yan, B. Jiu, H. Liu, B. Chen, and Z. Bao, "Prior knowledge-based simultaneous multibeam power allocation algorithm for cognitive multiple targets tracking in clutter," *IEEE Transactions on Signal Processing*, vol. 63, no. 2, pp. 512–527, 2014.

[16] J. Sun, W. Yi, P. K. Varshney, and L. Kong, "Resource scheduling for multi-target tracking in multi-radar systems with imperfect detection," *IEEE Transactions on Signal Processing*, vol. 70, pp. 3878–3893, 2022.

[17] P. Addabbo, S. Han, F. Biondi, G. Giunta, and D. Orlando, "Adaptive radar detection in the presence of multiple alternative hypotheses using kullback-leibler information criterion-part I: Detector designs," *IEEE Transactions on Signal Processing*, vol. 69, pp. 3730–3741, 2021.

[18] ——, "Adaptive radar detection in the presence of multiple alternative hypotheses using kullback-leibler information criterion-part II: Applications," *IEEE Transactions on Signal Processing*, vol. 69, pp. 3742–3754, 2021.

[19] C. Hao, D. Orlando, J. Liu, and C. Yin, *Advances in adaptive radar detection and range estimation*. Springer, 2022.

[20] H. Godrich, A. Haimovich, and R. S. Blum, "Target localisation techniques and tools for multiple-input multiple-output radar," *IET Radar, Sonar & Navigation*, vol. 3, no. 4, pp. 314–327, Aug. 2009.

[21] M. Dianat, M. R. Taban, J. Dianat, and V. Sedighi, "Target localization using least squares estimation for MIMO radars with widely separated antennas," *IEEE Transactions on Aerospace and Electronic Systems*, vol. 49, no. 4, pp. 2730–2741, Oct. 2013.

[22] H.-J. Shao, X.-P. Zhang, and Z. Wang, "Efficient closed-form algorithms for AOA based self-localization of sensor nodes using auxiliary variables," *IEEE Transactions on Signal Processing*, vol. 62, no. 10, pp. 2580–2594, 2014.

[23] C.-H. Park and J.-H. Chang, "Closed-form localization for distributed MIMO radar systems using time delay measurements," *IEEE Transactions on Wireless Communications*, vol. 15, no. 2, pp. 1480–1490, Oct. 2015.

[24] S. Zhao, X.-P. Zhang, X. Cui, and M. Lu, "Optimal two-way TOA localization and synchronization for moving user devices with clock drift," *IEEE Transactions on Vehicular Technology*, vol. 70, no. 8, pp. 7778–7789, 2021.

[25] P. K. Varshney, *Distributed detection and data fusion*. Springer Science & Business Media, 2012.

[26] R. Amiri, F. Behnia, and M. A. M. Sadr, "Exact solution for elliptic localization in distributed MIMO radar systems," *IEEE Transactions on Vehicular Technology*, vol. 67, no. 2, pp. 1075–1086, Oct. 2017.

[27] L. Yan, L. Pallotta, G. Giunta, and D. Orlando, "Robust target localization for multistatic passive radar networks," *IEEE Sensors Letters*, vol. 7, no. 7, pp. 1–4, 2023.

[28] J. Yan, H. Liu, B. Jiu, Z. Liu, and Z. Bao, "Joint detection and tracking processing algorithm for target tracking in multiple radar system," *IEEE Sensors Journal*, vol. 15, no. 11, pp. 6534–6541, 2015.

[29] J. Yan, H. Liu, W. Pu, H. Liu, Z. Liu, and Z. Bao, "Joint threshold adjustment and power allocation for cognitive target tracking in asynchronous radar network," *IEEE Transactions on Signal Processing*, vol. 65, no. 12, pp. 3094–3106, 2017.

[30] W. Liu, J. Liu, Y. Gao, G. Wang, and Y.-L. Wang, "Multichannel signal detection in interference and noise when signal mismatch happens," *Signal Processing*, vol. 166, p. 107268, 2020.

[31] W. Liu, J. Liu, C. Hao, Y. Gao, and Y.-L. Wang, "Multichannel adaptive signal detection: Basic theory and literature review," *Science China Information Sciences*, vol. 65, no. 2, p. 121301, 2022.

[32] Q. He, R. S. Blum, and A. M. Haimovich, "Noncoherent MIMO radar for location and velocity estimation: More antennas means better performance," *IEEE Transactions on Signal Processing*, vol. 58, no. 7, pp. 3661–3680, Mar. 2010.

[33] O. Bar-Shalom and A. J. Weiss, "Direct positioning of stationary targets using MIMO radar," *Signal Processing*, vol. 91, no. 10, pp. 2345–2358, Oct. 2011.

[34] R. Niu, R. S. Blum, P. K. Varshney, and A. L. Drozd, "Target localization and tracking in noncoherent multiple-input multiple-output radar systems," *IEEE Transactions on Aerospace and Electronic Systems*, vol. 48, no. 2, pp. 1466–1489, 2012.

[35] Q. He, N. H. Lehmann, R. S. Blum, and A. M. Haimovich, "MIMO radar moving target detection in homogeneous clutter," *IEEE Transactions on Aerospace and Electronic Systems*, vol. 46, no. 3, pp. 1290–1301, Aug. 2010.

[36] P. Wang, H. Li, and B. Himed, "Moving target detection using distributed MIMO radar in clutter with nonhomogeneous power," *IEEE Transactions on Signal Processing*, vol. 59, no. 10, pp. 4809–4820, Jun. 2011.

[37] J. Liu, H. Li, and B. Himed, "Persymmetric adaptive target detection with distributed MIMO radar," *IEEE Transactions on Aerospace and Electronic Systems*, vol. 51, no. 1, pp. 372–382, 2015.

[38] Y. Gao, H. Li, and B. Himed, "Knowledge-aided range-spread target detection for distributed MIMO radar in nonhomogeneous environments," *IEEE Transactions on Signal Processing*, vol. 65, no. 3, pp. 617–627, 2016.

[39] P. Wang and H. Li, "Target detection with imperfect waveform separation in distributed MIMO radar," *IEEE Transactions on Signal Processing*, vol. 68, pp. 793–807, Jan. 2020.
[40] S. Yang, Y. Lai, A. Jakobsson, and W. Yi, "Hybrid quantized signal detection with a bandwidth-constrained distributed radar system," *IEEE Transactions on Aerospace and Electronic Systems*, vol. 59, no. 6, pp. 7835–7850, 2023.
[41] G. Zhang, W. Yi, P. K. Varshney, and L. Kong, "Direct target localization with quantized measurements in non-coherent distributed MIMO radar systems," *IEEE Transactions on Geoscience and Remote Sensing*, vol. 61, pp. 1–18, 2023.
[42] S. Yang, W. Yi, and A. Jakobsson, "Multitarget detection strategy for distributed MIMO radar with widely separated antennas," *IEEE Transactions on Geoscience and Remote Sensing*, vol. 60, pp. 1–16, 2022.
[43] S. Zhang, Y. Zhou, M. Sha, L. Zhang, and L. Du, "Moving multitarget detection using a multisite radar system with widely separated stations," *Remote Sensing*, vol. 14, no. 11, p. 2660, 2022.
[44] A. Tajer, G. H. Jajamovich, X. Wang, and G. V. Moustakides, "Optimal joint target detection and parameter estimation by MIMO radar," *IEEE Journal of Selected Topics in Signal Processing*, vol. 4, no. 1, pp. 127–145, 2010.
[45] G. V. Moustakides, G. H. Jajamovich, A. Tajer, and X. Wang, "Joint detection and estimation: Optimum tests and applications," *IEEE Transactions on Information Theory*, vol. 58, no. 7, pp. 4215–4229, 2012.
[46] W. Yi, T. Zhou, Y. Ai, and R. S. Blum, "Suboptimal low complexity joint multi-target detection and localization for non-coherent MIMO radar with widely separated antennas," *IEEE Transactions on Signal Processing*, vol. 68, pp. 901–916, 2020.
[47] Y. Lai, L. Venturino, E. Grossi, and W. Yi, "Joint detection and localization in distributed MIMO radars employing waveforms with imperfect auto- and cross-correlation," *IEEE Transactions on Vehicular Technology*, vol. 72, no. 12, pp. 16 524–16 537, 2023.
[48] L. Zhu, G. Wen, Y. Liang, D. Luo, and H. Song, "Energy-guided multitarget detection and localization for distributed MIMO radar: Analysis and solution," *IEEE Transactions on Aerospace and Electronic Systems*, vol. 59, no. 1, pp. 82–97, 2022.
[49] L. Zhu, G. Wen, Y. Liang, D. Luo, and H. Jian, "Multitarget enumeration and localization in distributed MIMO radar based on energy modeling and compressive sensing," *IEEE Transactions on Aerospace and Electronic Systems*, vol. 59, no. 4, pp. 4493–4510, 2023.
[50] D. Orlando and G. Ricci, "Adaptive radar detection and localization of a point-like target," *IEEE Transactions on Signal Processing*, vol. 59, no. 9, pp. 4086–4096, 2011.
[51] A. Aubry, A. De Maio, G. Foglia, C. Hao, and D. Orlando, "Radar detection and range estimation using oversampled data," *IEEE Transactions on Aerospace and Electronic Systems*, vol. 51, no. 2, pp. 1039–1052, 2015.
[52] A. Aubry, A. De Maio, S. Marano, and M. Rosamilia, "Single-pulse simultaneous target detection and angle estimation in a multichannel phased array radar," *IEEE Transactions on Signal Processing*, vol. 68, pp. 6649–6664, Nov. 2020.
[53] T. Wang, C. Yin, D. Xu, C. Hao, D. Orlando, and G. Ricci, "Joint detection and delay-doppler estimation algorithms for mimo radars," *IEEE Transactions on Signal Processing*, 2024.
[54] D. Slepian, "On bandwidth," *Proceedings of the IEEE*, vol. 64, no. 3, pp. 292–300, Mar. 1976.
[55] J. Liu, Z.-J. Zhang, Y. Cao, and S. Yang, "A closed-form expression for false alarm rate of adaptive MIMO-GLRT detector with distributed MIMO radar," *Signal Processing*, vol. 93, no. 9, pp. 2771–2776, 2013.
[56] P. Stoica and Y. Selen, "Model-order selection: a review of information criterion rules," *IEEE Signal Processing Magazine*, vol. 21, no. 4, pp. 36–47, Jul. 2004.
[57] P. Stoica, Y. Selen, and J. Li, "On information criteria and the generalized likelihood ratio test of model order selection," *IEEE Signal Processing Letters*, vol. 11, no. 10, pp. 794–797, Oct. 2004.
[58] Y. Lai, G. Zhang, S. Yang, W. Yi, and L. Kong, "A quantization based censoring detection method with limited communication rates for distributed MIMO radar," in *2021 CIE International Conference on Radar (Radar)*. IEEE, 2021, pp. 1188–1191.

Yangming Lai (Student Member, IEEE) received the B.E. degree in electronic engineering from the University of Electronic Science and Technology of China, Chengdu, China, in 2018, where he is currently working toward the Ph.D. degree in information and communication engineering. From October 2022 to October 2023, he was a Visiting Ph.D. Student with the Communication Systems Group, Department of Electrical Engineering, Chalmers University of Technology, Gothenburg, Sweden, under the financial support from the China Scholarship Council. His research interests include statistical signal processing, radar signal processing, and joint radar-communications, especially target detection and localization technology.

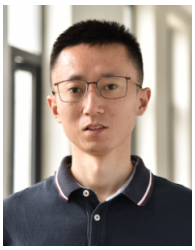

Wei Yi (Senior Member, IEEE) received the B.E. and Ph.D. degrees in electronic engineering from the University of Electronic Science and Technology of China, Chengdu, China, in 2006 and 2012, respectively. From 2010 to 2012, he was a Visiting Student with the Melbourne Systems Laboratory, University of Melbourne, Melbourne, VIC, Australia.

Since 2012, he has been with the University of Electronic Science and Technology of China, where he is currently a Full Professor with the School of Information and Communication Engineering. His research interests include target detection and tracking, radar signal processing, multi-sensor information fusion, and resources management.

Dr. Yi was the recipient of the Best Student Paper Competition-First place award at the 2012 IEEE Radar Conference, Atlanta, Best Student Paper Award at the 15th FUSION Conference, Singapore, 2012. He is the Associate Editor of *IEEE Transactions on Signal Processing*, and a Member of the Editorial Boards of the *Journal of Radars*, the *MDPI Sensors*. He was also the General Co-Chair of ICCAIS 2019 and a Technical Program Committee Member of international conferences, such as IEEE Radar Conference and FUSION Conference.

Henk Wymeersch (Fellow, IEEE) obtained the Ph.D. degree in Electrical Engineering/Applied Sciences in 2005 from Ghent University, Belgium. He is currently a Professor of Communication Systems with the Department of Electrical Engineering at Chalmers University of Technology, Sweden. Prior to joining Chalmers, he was a postdoctoral researcher from 2005 until 2009 with the Laboratory for Information and Decision Systems at the Massachusetts Institute of Technology. Prof. Wymeersch served as Associate Editor for IEEE Communication Letters (2009-2013), IEEE Transactions on Wireless Communications (since 2013), and IEEE Transactions on Communications (2016-2018) and is currently Senior Member of the IEEE Signal Processing Magazine Editorial Board. During 2019-2021, he was an IEEE Distinguished Lecturer with the Vehicular Technology Society. His current research interests include the convergence of communication and sensing, in a 5G and Beyond 5G context.

Musa Furkan Keskin (Member, IEEE) received the Ph.D. degree from the Department of Electrical and Electronics Engineering, Bilkent University, Ankara, Turkey in 2018. He is currently Research Specialist with the department of Electrical Engineering at Chalmers University of Technology, Gothenburg, Sweden, contributing to many interdisciplinary and industry-focused research projects at Swedish and European level in the area of integrated localization, communication and sensing in 6G systems. His current research interests include integrated sensing and communications, localization and sensing with distributed arrays, and hardware impairment mitigation and exploitation in beyond 5G/6G systems.

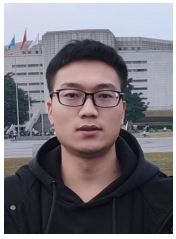

Qiyu Zhou (Student Member, IEEE) received the B.S. degree from the Zhongyuan University of Technology, Zhengzhou, China, in 2018. He is currently pursuing the Ph.D. degree with the School of Information and Communication Engineering, University of Electronic Science and Technology of China (UESTC), Chengdu, China. His research interests include statistical signal processing, radar signal processing, and passive radar localization technology.

Lingjiang Kong (Senior Member, IEEE) was born in 1974. He received the B.S. degree in electronic engineering and the M.S. and Ph.D. degrees in signal and information processing from the University of Electronic Science and Technology of China (UESTC), Chengdu, China, in 1997, 2000, and 2003, respectively. From September 2009 to March 2010, he was a Visiting Researcher with the University of Florida, Gainesville, FL, USA. He is currently a Professor with the School of Information and Communication Engineering, UESTC. His research interests include multiple-input multiple-output radar, through the wall radar, and statistical signal processing.